

UC Riverside

2019 Publications

Title

Cu

²

O Photocathode with Faster Charge Transfer by Fully Reacted Cu Seed Layer to Enhance Performance of Hydrogen Evolution in Solar Water Splitting Applications

Permalink

<https://escholarship.org/uc/item/46k2g8dd>

Journal

ChemCatChem, 11(17)

ISSN

1867-3880 1867-3899

Authors

Jung, Kichang

Lim, Taehoon

Bae, Hyojung

et al.

Publication Date

2019-07-24

DOI

10.1002/cctc.201900526

Peer reviewed

Cu₂O Photocathode with Faster Charge Transfer by Fully Reacted Cu Seed Layer to Enhance Performance of Hydrogen Evolution in Solar Water Splitting Applications

Kichang Jung,^[a, b] Taehoon Lim,^[a] Hyojung Bae,^[c, d] Jun-Seok Ha,^[c, d] and Alfredo A. Martinez-Morales*^[a, b, e]

In this work, we study the effect of Cu₂O film obtained from a fully reacted Cu seed layer as a photoelectrode in photoelectrochemical cells. The full reaction of the Cu layer shows an enhanced photocurrent density and improved efficiency in hydrogen evolution. The photocurrent density of textured Cu₂O (0.58 mA cm⁻² at 0 V vs. RHE), without an unreacted Cu layer is two times higher than films containing an unreacted Cu layer (0.29 mA cm⁻² at 0 V vs. RHE), under AM 1.5 illumination (100 mW cm⁻²). The thickness of the unreacted Cu layer

influences significantly the charge transfer process at the interface between the Cu₂O and electrolyte. The enhanced photoelectrochemical performance of textured Cu₂O is attributed to the reduced charge recombination resulting from a longer carrier lifetime in the Cu₂O layer. Experimentally we confirmed that the unreacted Cu layer inhibits the photoelectrochemical performance of Cu₂O-based photocathodes. The elimination of the unreacted Cu layer leads to higher photocurrent density.

Introduction

Hydrogen is a promising renewable fuel with the potential to be used as an energy source to alleviate the higher demand for energy driven by population growth. Hydrogen has a high mass energy density and is an eco-friendly material. These two characteristics make it an attractive energy source for addressing current and future energy needs.^[1] The efficient and cost-effective harvesting and storing of hydrogen gas are critical for its utilization across various fields and applications.^[2,3] The use of photoelectrochemical (PEC) cells for water splitting applications as a method to efficiently harvest hydrogen gas using solar energy has been carried out extensively by various research groups.^[4-6] PEC cells convert sunlight to chemical

energy by splitting water molecules for generating hydrogen gas.^[6-9] Therefore, research focused in improving the efficiency in PEC cells is imperative to make hydrogen a more competitive technology. Among materials used to produce hydrogen gas using PEC cells, Cu₂O is a good candidate because it is cost-competitive and an abundant material in the earth.^[10-15] Cu₂O is a p-type semiconductor material with a band gap of 1.6–2.2 eV, absorbance in the visible light range (563–775 nm), and a suitable band edge alignment that is amenable for generating chemical energy.^[16-18] In a PEC device, the absorbed sunlight at the Cu₂O surface generates excited electrons by reducing protons to hydrogen gas at the interface between the photoelectrode and the electrolyte.^[10,11,13-15]

Cu₂O has a theoretical hydrogen conversion efficiency of 18% in PEC cells and a power conversion efficiency of 20% in a solar cell.^[12,15] However, low hydrogen generation and instability are two challenges that prevent the usage of Cu₂O as a photocathode in PEC cells.^[19] The low efficiency is attributed to the high charge recombination caused by the slow carrier transfer rate at the Cu₂O surface.^[20] To increase the efficiency of Cu₂O, a thick film around 10 μm is necessary for the effective absorption of sunlight.^[21,22] However, minority carrier (electrons) in the Cu₂O reacting with protons have less than a 200 nm diffusion length, resulting in an inefficient reaction.^[23] The charge diffusion length and the carrier transfer rate are important factors to improve the efficiency of hydrogen gas generated from excited electrons.^[24] In the literature, the properties of Cu₂O have been engineered for increasing the charge diffusion length and improving the carrier transfer rate as well. There are various research methods to improve Cu₂O performance such as doping,^[25] high temperature processing for enhancing the crystal quality,^[11] engineering an overlayer,^[12,26-28] and modifying the morphology to reduce the electron pathway length.^[29,30] Despite these efforts to improve


[a] K. Jung, T. Lim, Prof. A. A. Martinez-Morales
College of Engineering- Center for Environmental Research & Technology
University of California, Riverside
1084 Columbia Ave., Riverside CA 92507 (USA)
E-mail: alfmart@ece.ucr.edu

[b] K. Jung, Prof. A. A. Martinez-Morales
Department of Chemical and Environmental Engineering
University of California, Riverside
900 University Ave., Riverside CA 92521 (USA)

[c] H. Bae, Prof. J.-S. Ha
Optoelectronics Convergence Research Center
Chonnam National University
77 Yongbong-ro, Buk-gu, Gwangju, 61186 (Republic of Korea)

[d] H. Bae, Prof. J.-S. Ha
School of Chemical Engineering
Chonnam National University
77 Yongbong-ro, Buk-gu, Gwangju, 61186
Republic of Korea

[e] Prof. A. A. Martinez-Morales
Materials Science and Engineering Program
University of California, Riverside
900 University Ave., Riverside CA 92521 (USA)

 Supporting information for this article is available on the WWW under <https://doi.org/10.1002/cctc.201900526>

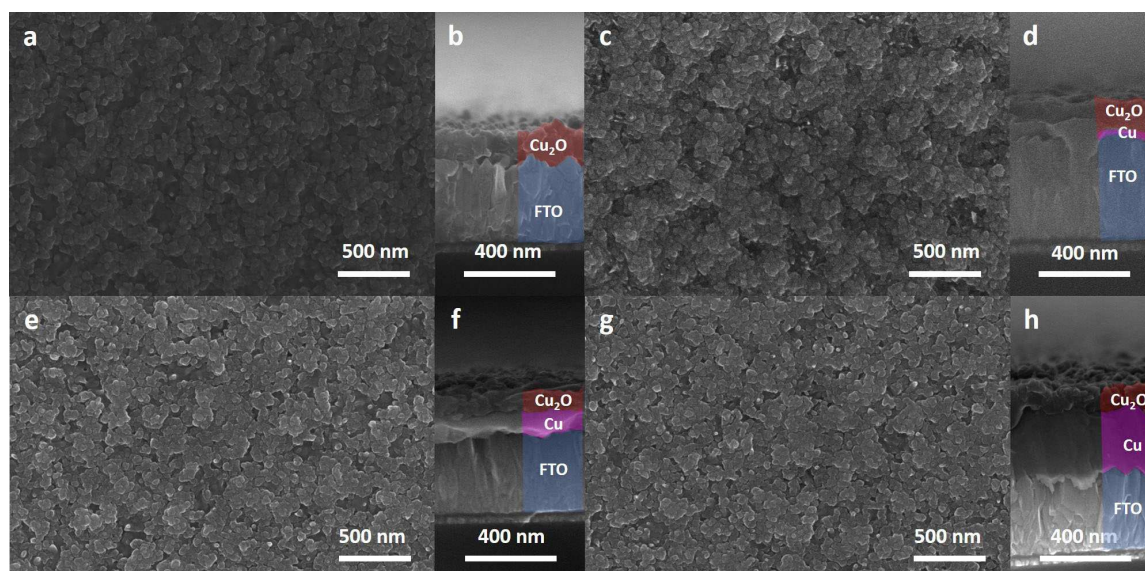


Figure 1. Comparison of Cu_2O samples with different Cu seed layer thickness. (a), (c), (e) and (g) top view. (b), (d), (f), and (h) cross-sectional SEM images of the samples synthesized from 100, 200, 300, and 500 nm samples, respectively.

the generation efficiency, the utilization of Cu_2O still requires more research to improve its low photocurrent density in PEC cells.

In this paper, we report the improved hydrogen generation properties of textured Cu_2O photocathode film, via the full reaction of the Cu seed layer between the Cu_2O and the fluorine doped tin oxide (FTO) substrate. The textured Cu_2O has a higher PEC efficiency due to its larger surface area compared to thin-film structures. Via our solution base synthesis method, we successfully synthesized a textured Cu_2O film on FTO substrate from a Cu seed layer film. When Cu_2O is used as a photo-electrode, any unreacted Cu greatly impacts the hole transfer in the PEC cell. In this work, the relationship between electron/hole recombination and carrier transfer rate is investigated. Photoelectrochemical reaction measurements are analyzed to determine the reaction at the interface between Cu_2O and electrolyte. The material properties are characterized in terms of their morphology, crystallinity, and light absorbance.

Results and Discussion

Four samples with different thickness are synthesized via a solution method. The synthesized samples show a textured Cu_2O film on the FTO substrate as observed by scanning electron microscopy (SEM) characterization (shown in Figure 1). The morphology of these samples is rougher than the CuO layer synthesized on FTO substrate by thermally oxidizing the Cu seed layer (Figure S1). In contrast to the CuO film which maintains the FTO surface topography, the Cu_2O forms a morphology that is independent of the FTO substrate. The samples show that the textured Cu_2O films have a peak to peak distance around 80 nm (Figure S2 and S3). Although the thickness of the Cu seed layer is different for each sample, the

atomic force microscopy (AFM) topography results show a similar root mean square roughness value for all samples, ranging from 17 to 20 nm. This is evidence that the synthesized Cu_2O films on the FTO substrate have a similar morphology regardless of the starting Cu seed layer thickness. However, the cross-sectional SEM images show that the resulting thickness of the Cu_2O layer on the FTO substrate is limited by the reaction time of solution-based synthesis process (shown in Table 1).

Table 1. Thickness of target Cu seed layer and measured Cu_2O on FTO substrate after annealing process.

	Target Cu seed layer [nm]	Measured $\text{Cu}_2\text{O}^{[a]}$ [nm]
Sample 1	100	114 ± 28
Sample 2	200	132 ± 33
Sample 3	300	114 ± 21
Sample 4	500	137 ± 41

[a] Deviation calculated by ImageJ.

The combined thickness of the unreacted Cu and textured Cu_2O is dependent to the starting Cu seed layer thickness as shown in Figure S4. Particularly, double layers are observed for samples 2, 3, and 4, whereas a single layer is observable for sample 1. The unreacted layer thickness between the Cu_2O top layer and FTO is 115 and 300 nm in sample 3 and 4, respectively. Through SEM morphology analysis, we conclude that while the synthesized Cu_2O films have different thickness because of the unreacted layer, in all instances textured Cu_2O films possessing similar morphology are synthesized successfully.

The crystallinity of the synthesized samples is analyzed by X-ray diffraction (XRD) characterization from $2\theta = 35^\circ$ to 60° , as shown in Figure 2. The peaks for Cu_2O , Cu, and FTO are labelled

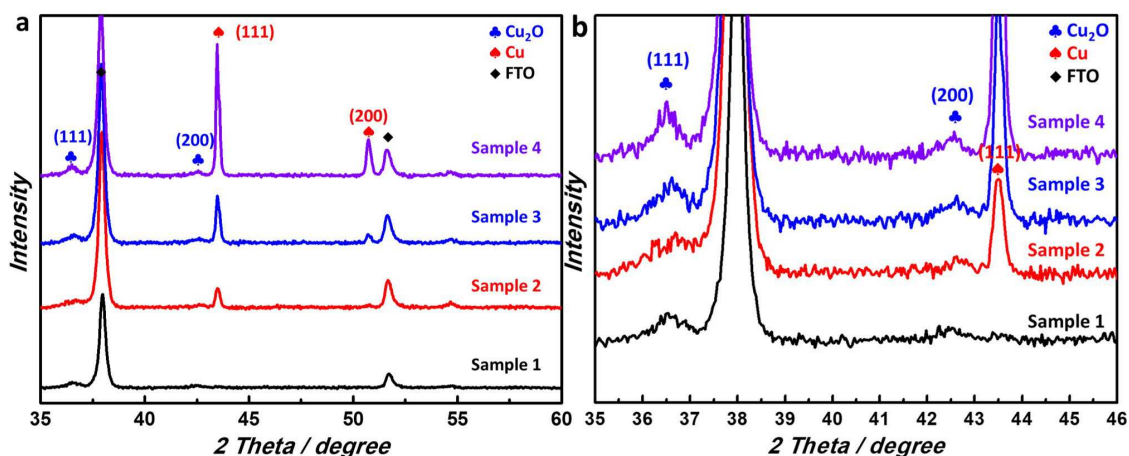


Figure 2. X-ray diffraction patterns of samples with and without the unreacted Cu layer with indexes taken from JCPDS: Cu₂O #05-0667, Cu #04-0836, FTO #41-1445 (a) from $2\theta = 35^\circ$ to 60° and (b) from $2\theta = 35^\circ$ to 46° .

with their corresponding crystal planes. All samples show the peaks for Cu₂O (111) and (020) crystal planes. On the other hand, sample 2, 3, and 4 show two additional peaks at $2\theta = 43.5^\circ$ and 51.6° , corresponding to the cubic Cu (111) and (200) crystal planes (JCPDS 04-0836). Intensity of the Cu peaks increase with increasing thickness of the unreacted Cu seed layer, while the intensity of the Cu₂O peaks remained unchanged. These results are in support of the observations from cross-sectional SEM analysis. The unreacted layer between Cu₂O and FTO is the Cu layer identified in the XRD results. All the synthesized samples show a textured Cu₂O film with similar crystallinity, irrespective of the unreacted Cu layer thickness between Cu₂O and FTO substrate.

Optical properties of the synthesized samples are analyzed by UV-Vis-NIR spectroscopy. The absorption spectra versus wavelength are shown in Figure 3. There are specific absorption peaks at 680 and 640 nm wavelength for sample 1 and 2,

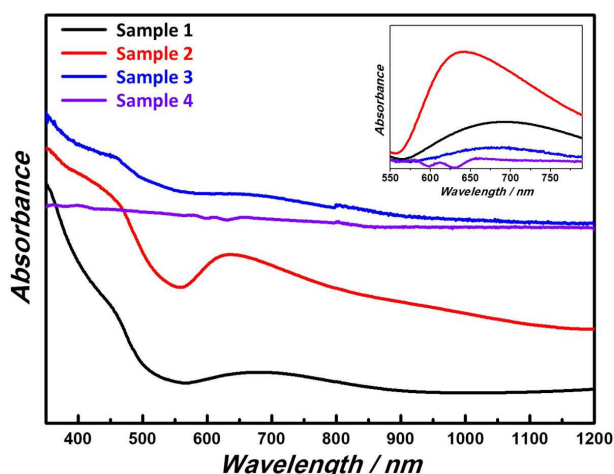


Figure 3. The absorption spectra in the range of UV/Vis/NIR of samples with and without the unreacted Cu layer. The inserted spectra shows the absorbance of the samples after subtracting the baseline.

respectively. Both are absorption peaks by the Cu₂O layer, verified by the bandgap (1.6 to 2.2 eV) of Cu₂O with an absorption wavelength range from 563 to 775 nm. The obtained bandgap is in the range of reported values in the literature.^[16-18] Even though sample 3 and 4 have a Cu₂O layer with similar thickness, the absorption peak by the Cu₂O layer in sample 4 is not noticeable. In sample 3, the absorption peak by Cu₂O can be weakly observed (Figure 3 inset). Moreover, sample 4 shows a plateau for the entire range, indicative that the unreacted thick Cu layer with 300 nm prohibits light penetration from the top layer to the FTO substrate. The absorption intensity from unreacted Cu layer increases with thicker unreacted Cu layer thickness as observed in samples 3 and 4. Additionally, sample 2 has a higher absorption peak intensity than sample 1. These results point out to the absorption properties of the Cu₂O/Cu/FTO structure being dominated by the Cu layer thickness, which blocks the incoming light when the seed layer is thicker than 100 nm.

The performance of the textured Cu₂O film as the photocathode in PEC cells is measured. The photocurrent density is measured under illumination to analyze the photocatalytic operation of the photocathode, as shown Figure 4. The highest photocurrent density 0.58 mA cm^{-2} at 0 V vs RHE is achieved from sample 1 photocathode under illumination. On the other hand, both sample 3 and 4 show the lowest photocurrent density among the synthesized samples. This is attributed to the unreacted Cu layer (thicker than 100 nm) that reduces photocurrent density. The unreacted Cu layer acts as a carrier blocking layer between Cu₂O and FTO. Therefore, the unreacted Cu layer negatively impacts the separation and transportation of the electrons and holes generated from the Cu₂O layer. Sample 2 shows a reduced performance compared to sample 1 due to a very thin unreacted Cu layer characterized by XRD spectra at $2\theta = 42.7^\circ$, that affects the photocurrent density irrespective of the amount of absorbed light at the Cu₂O layer. In order to enhance the photocurrent density, a textured Cu₂O

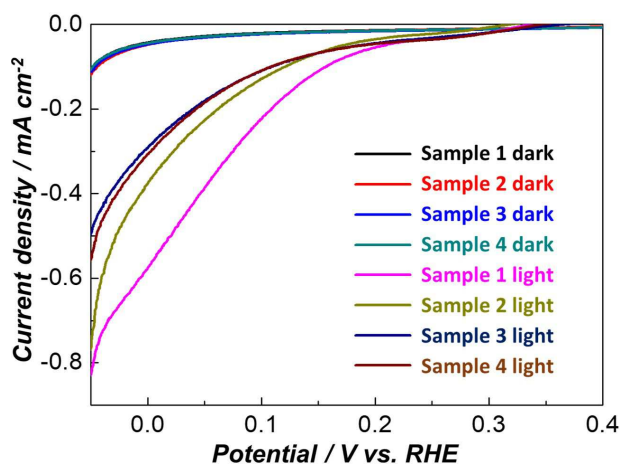


Figure 4. Photoelectrochemical performance measurement (J - V curve) under dark and illuminated conditions (AM 1.5 G, 100 mW cm^{-2}).

film without the unreacted Cu layer must be synthesized, as demonstrated by the sample 1.

Electrochemical impedance spectroscopy (EIS) is used to study the interface reaction between the photoelectrode and the electrolyte in the fabricated PEC cells. The EIS measurements are conducted under illumination in a frequency range from 10^5 to 10^{-1} Hz, with an amplitude of 10 mV at an open circuit potential. Nyquist plots for the samples are presented in Figure 5. The charge transfer process is expressed as a semi-circle in the Nyquist plot. The diameter of the semicircle in a Nyquist plot is equal to the charge transfer resistance (R_{ct}), shown in Table 2. The R_{ct} increases with the unreacted Cu layer thickness under illumination. The decrease in electron conductivity is affected by the unreacted Cu layer at the photocathode/FTO interface. Even in the case when the thin unreacted Cu layer is not distinguishable by cross-sectional SEM analysis it increases the R_{ct} . Sample 3 and 4 with an unreacted

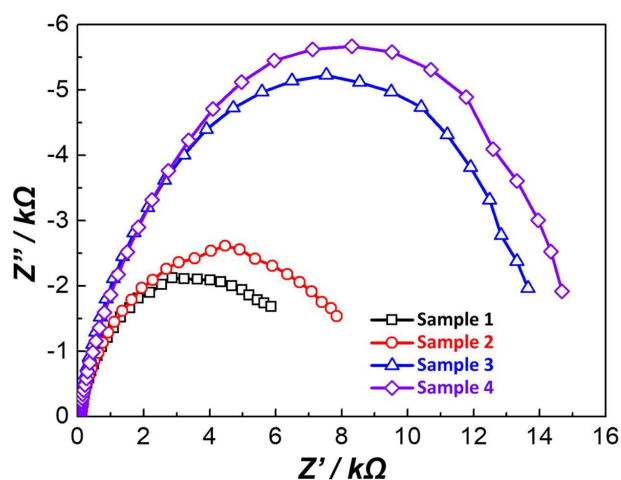


Figure 5. Nyquist plots of samples based on photocathodes under illumination (AM 1.5G, 100 mW cm^{-2} , 10 mV open circuit potential, 10^2 - 10^{-1} Hz frequency range, 0.1 M Na_2SO_4).

Table 2. The charge transfer resistance (R_{ct}), carrier density (N_A), flatband potential (V_{fb}), and carrier lifetime (τ) measured and calculated from the fitting parameters from Nyquist, Mott-Schottky, and Bode plots from the samples.

Sample	R_{ct} [Ω]	N_A [cm^{-3}]	V_{fb} [V]	τ [ms]
1	7.7×10^3	2.74×10^{15}	0.492	13.4
2	8.9×10^3	3.04×10^{15}	0.486	2.9
3	14.5×10^3	2.17×10^{15}	0.496	3.3
4	15.9×10^3	2.97×10^{15}	0.486	3.5

Cu layer thicker than 100 nm show two times higher R_{ct} than sample 1 and 2. The results show that the unreacted Cu layer between Cu_2O and FTO reduces the charge transfer process at the interface between Cu_2O surface and electrolyte. This is because the generated carriers cannot be effectively separated and recombine before can be collected. The capacitance on the photoelectrode/electrolyte are measured in order to calculate the flat band potential (V_{fb}) and carrier density (N_A), shown in Figure 6.

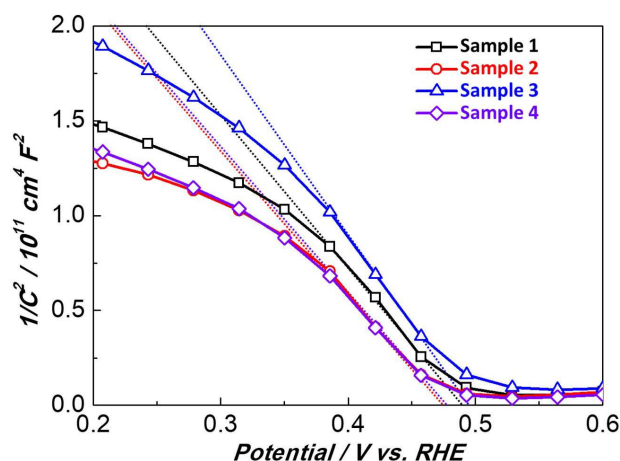


Figure 6. Mott-Schottky plots of samples (10^3 Hz frequency, 0.1 M Na_2SO_4).

Parameters are calculated from $1/C^2$ vs. applied potential plot (Mott-Schottky plot) at a fixed frequency of 10^3 Hz. The measured $1/C^2$ is expressed in the Equation (1) below:

$$\frac{1}{C^2} = \frac{2}{N_A e \epsilon_0 \epsilon} \left[(V_s - V_{fb}) - \frac{kT}{e} \right] \quad (1)$$

N_A , e , ϵ_0 , ϵ , k , T and V_s are the hole density, the elementary charge, the permittivity of the vacuum, the relative permittivity of photocathode (Cu_2O is 10.26), the Boltzmann constant, temperature, and the applied potential, respectively.^[1,15] Based on this equation, the hole density in the Cu_2O layer can be calculated from the slope of the curve. The carrier density of the samples ranges from 2.17×10^{15} to $3.04 \times 10^{15} \text{ cm}^{-3}$, shown in Table 2. The tangential point from the extrapolated linear part of the curve is the V_{fb} of the photocathode. The negative slope of the linear part in the curve shows p-type semi-

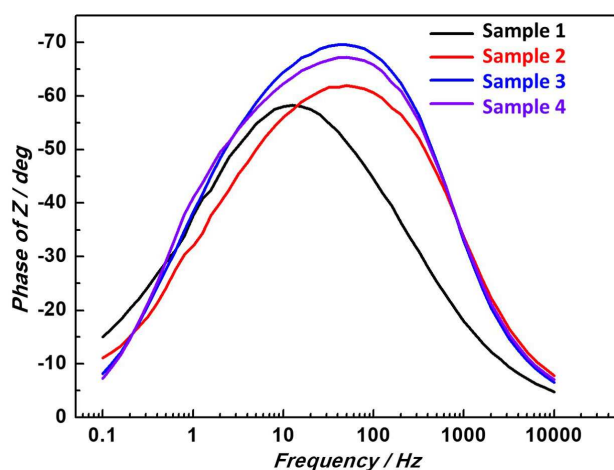


Figure 7. Bode plot of samples under illumination (AM 1.5 G, 100 mW cm⁻²).

conductor behavior. The V_{fb} is 0.486 to 0.496 V vs. RHE. These results indicate that the unreacted Cu layer does not affect the carrier density and V_{fb} .

Moreover, the Bode plot displaying the phase as the response against the frequencies endow the information of the carrier transport/recombination process in the semiconductor (Figure 7). The Bode plot determines the information of carrier lifetime (τ) inside the PEC under illumination. Measured frequencies at the maximum phase were used to calculate the carrier lifetimes $\tau = 1/2\pi f_{max}$.^[31–33] The hole lifetime decreases significantly with the existence of the unreacted Cu layer. Longer carrier lifetime (13.5 ms) is obtained in sample 1. The three samples with an unreacted Cu layer show shorter carrier lifetime ranging from 2.9 to 3.5 ms. The PEC cell using sample 1 achieved the best efficiency among the samples due to the longer carrier lifetime that leads to a slow recombination rate. The Cu₂O film without the unreacted Cu layer improve the carrier lifetime while its carrier density and V_{fb} are not affected (Figure S5). From our analysis, we conclude that the enhanced photocurrent density using Cu₂O is attributed to the longer carrier lifetime.

Conclusions

Cu₂O photocathodes with fully reacted Cu layer have been developed via a solution based process. These samples show superior electrochemical properties in PEC cells compared to samples with an unreacted Cu layer. A 100% enhancement in photocurrent density under sunlight illumination for a water splitting application is measured. We confirmed that the enhancement is attributed to the improvement in the charge transfer rate and carrier lifetime. Therefore, the sample with fully reacted Cu layer presents low charge transfer resistance at the interface between the Cu₂O surface and electrolyte.

Experimental Section

Materials and Methods

All chemicals in this paper are purchased from Sigma Aldrich. FTO on glass substrate (surface resistivity $\sim 13 \Omega/\text{sq}$, Sigma Aldrich) is used as a substrate. FTO is cleaned using a detergent solution in deionized (DI) water, acetone, and isopropyl alcohol (IPA) in an ultrasonication bath for 5 min for each step. A nitrogen gun is used to dry the FTO after the IPA rinse. A Cu seed layer is deposited by e-beam evaporation on the FTO substrate patterned with a 1 x 1 cm² window. The deposition rate is maintained at less than 1.2 Å/sec. Various Cu film thicknesses are deposited. These samples are denoted sample 1, 2, 3, and 4. The solution for making the textured Cu₂O is prepared as detailed by Chattopadhyay's group.^[10] The initial solution is mixed with 0.038 M ammonium persulfate ((NH₄)₂S₂O₈) and 0.191 M sodium hydroxide (NaOH). The reaction solution is prepared by adding 4 ml in 160 ml DI water. The solution is stirred until fully mixed. The prepared samples with Cu seed layer are dipped into the solution for 1 h at room temperature without stirring. The residue on the surface of sample is rinsed by DI water for 5 min and dried by nitrogen gun. The samples are annealed by rapid thermal annealing at 550 °C for 1 min under nitrogen condition. In order to compare the surface morphology of a flat uniform film (as a control sample), a Cu film on FTO glass is thermally oxidized at 600 °C for 1 h under air.

Materials Characterization

The morphology of the synthesized materials on the FTO glass are characterized by scanning electron microscopy (SEM, FEI NovaNanoSEM450) and atomic force microscopy (AFM, MFP-3D from Asylum Research). Crystallinity of the samples is analyzed by X-ray diffraction (XRD, PANalytical X'Pert X-ray diffractometer) using Cu K α radiation (1.540598 Å). Optical properties are measured by double beam scanning UV-Vis-NIR spectrophotometry (Varian Cary 500).

Photoelectrochemical Measurements

Photoelectrochemical performance of the synthesized samples, as photocathodes for PEC devices, is measured by a potentiostat with a 3-electrode setup using Ag/AgCl/KCl as the reference electrode, Pt wire as the counter electrode, and the synthesized film as the working electrode. 0.1 M Na₂SO₄ electrolyte solution is used for the testing of the PEC. A solar simulator (Newport, Oriel Sol3A Class AAA Solar Simulator, 450 W Xenon) is used as the light source (AM 1.5 G, 100 mW cm⁻²). The solar simulator was calibrated by a monoclinic silicon solar cell (Newport, Oriel[®] Reference Solar Cell & Meter, 91150 V). The scan rate for the linear sweep voltammetry is 0.05 V/s and the applied potential is -0.05 to 0.4 V vs. RHE. Electrochemical impedance spectroscopy (EIS) is conducted at open circuit potential from 10⁵ to 10⁻¹ Hz frequency under illumination to study interfacial charge transfer between the photocathode and the electrolyte. Measuring the capacitance against potential at 10³ Hz frequency is performed under dark from 0.2 to 0.6 V vs RHE to characterize the V_{fb} .

Notes

The authors declare no competing financial interest.

Acknowledgements

Electron microscopy was performed on the Nova NanoSEM450 in CFAMM at UC Riverside. This research was partially supported by a grant from UC Solar (MR-15-328386).

Conflict of Interest

The authors declare no conflict of interest.

Keywords: Hydrogen evolution · Photoelectrocatalyst · Cu₂O · metal-oxide catalyst · photocatalyst

- [1] Z. Zhang, P. Wang, *J. Mater. Chem.* **2012**, *22*, 2456–2464.
- [2] A. Choudhury, H. Chandra, A. Arora, *Renew. Sust. Energ. Rev.* **2013**, *20*, 430–442.
- [3] A. Qi, B. Peppley, K. Karan, *Fuel Process. Technol.* **2007**, *88*, 3–22.
- [4] D. Kim, K. K. Sakimoto, D. Hong, P. Yang, *Angew. Chem. Int. Ed. Engl.* **2015**, *54*, 3259–3266.
- [5] F. E. Osterloh, *Chem. Soc. Rev.* **2013**, *42*, 2294–2320.
- [6] I. S. Cho, C. H. Lee, Y. Feng, M. Logar, P. M. Rao, L. Cai, D. R. Kim, R. Sinclair, X. Zheng, *Nat. Commun.* **2013**, *4*, 1723.
- [7] X. Wang, R. Long, D. Liu, D. Yang, C. Wang, Y. Xiong, *Nano Energy* **2016**, *24*, 87–93.
- [8] Q. Wang, T. Hisatomi, Q. Jia, H. Tokudome, M. Zhong, C. Wang, Z. Pan, T. Takata, M. Nakabayashi, N. Shibata, *Nat. Mater.* **2016**, *15*, 611–615.
- [9] O. Khaselev, J. A. Turner, *Science* **1998**, *280*, 425–427.
- [10] A. Paracchino, N. Mathews, T. Hisatomi, M. Stefik, S. D. Tilley, M. Grätzel, *Energ. Environ. Sci.* **2012**, *5*, 8673–8681.
- [11] Y.-K. Hsu, C.-H. Yu, Y.-C. Chen, Y.-G. Lin, *Electrochim. Acta* **2013**, *105*, 62–68.
- [12] T. Minami, T. Miyata, Y. Nishi, *Sol. Energy* **2014**, *105*, 206–217.
- [13] D. Chen, Z. Liu, Z. Guo, W. Yan, Y. Xin, *J. Mater. Chem. A* **2018**, *6*, 20393–20401.
- [14] A. A. Dubale, C.-J. Pan, A. G. Tamirat, H.-M. Chen, W.-N. Su, C.-H. Chen, J. Rick, D. W. Ayele, B. A. Aragaw, J.-F. Lee, *J. Mater. Chem. A* **2015**, *3*, 12482–12499.
- [15] J. Luo, L. Steier, M.-K. Son, M. Schreier, M. T. Mayer, M. Grätzel, *Nano Lett.* **2016**, *16*, 1848–1857.
- [16] A. Kargar, S. S. Partokia, M. T. Niu, P. Allameh, M. Yang, S. May, J. S. Cheung, K. Sun, K. Xu, D. Wang, *Nanotechnology* **2014**, *25*, 205401.
- [17] A. A. Dubale, A. G. Tamirat, H.-M. Chen, T. A. Berhe, C.-J. Pan, W.-N. Su, B.-J. Hwang, *J. Mater. Chem. A* **2016**, *4*, 2205–2216.
- [18] S. Jamali, A. Moshaii, *Appl. Surf. Sci.* **2017**, *419*, 269–276.
- [19] K. L. Sowers, A. Fillinger, *J. Electrochem. Soc.* **2009**, *156*, F80–F85.
- [20] Y. Yang, D. Xu, Q. Wu, P. Diao, *Sci. Rep.* **2016**, *6*, 35158.
- [21] A. Paracchino, V. Laporte, K. Sivula, M. Grätzel, E. Thimsen, *Nat. Mater.* **2011**, *10*, 456–461.
- [22] C. J. Engel, T. A. Polson, J. R. Spado, J. M. Bell, A. Fillinger, *J. Electrochem. Soc.* **2008**, *155*, F37–F42.
- [23] A. Paracchino, J. C. Brauer, J.-E. Moser, E. Thimsen, M. Grätzel, *J. Phys. Chem. C* **2012**, *116*, 7341–7350.
- [24] K. P. Musselman, A. Marin, L. Schmidt-Mende, J. L. MacManus-Driscoll, *Adv. Funct. Mater.* **2012**, *22*, 2202–2208.
- [25] L. Zhang, D. Jing, L. Guo, X. Yao, *ACS Sustain. Chem. Eng.* **2014**, *2*, 1446–1452.
- [26] T. Minami, Y. Nishi, T. Miyata, *Appl. Phys. Express* **2013**, *6*, 044101.
- [27] Z. Zhang, R. Dua, L. Zhang, H. Zhu, H. Zhang, P. Wang, *ACS Nano* **2013**, *7*, 1709–1717.
- [28] C. G. Morales-Guio, S. D. Tilley, H. Vrubel, M. Grätzel, X. Hu, *Nat. Commun.* **2014**, *5*, 3059.
- [29] K.-S. Choi, *J. Phys. Chem. Lett.* **2010**, *1*, 2244–2250.
- [30] Y. Qu, J. Qian, J. Liu, L. Yao, L. Zhao, X. Song, P. Zhang, L. Gao, *J. Electrochem. Soc.* **2019**, *166*, H452–H458.
- [31] K.-M. Lee, C.-W. Hu, H.-W. Chen, K.-C. Ho, *Sol. Energy. Mat. Sol. C.* **2008**, *92*, 1628–1633.
- [32] H. Shelke, A. Lokhande, A. Patil, J. Kim, C. Lokhande, *Surfaces and Interfaces* **2017**, *9*, 238–244.
- [33] S. S. Patil, N. L. Tarwal, H. M. Yadav, S. D. Korade, T. S. Bhat, A. M. Teli, M. M. Karanjkar, J. H. Kim, P. S. Patil, *J. Solid State Electr.* **2018**, *22*, 3015–3024.

Manuscript received: March 27, 2019

Revised manuscript received: May 28, 2019

Accepted manuscript online: June 19, 2019

Version of record online: July 24, 2019